A Novel Beta Parameter Based Fuzzy-Logic Controller for Photovoltaic MPPT Application

Xingshuo Li, Huiqing Wen, Yihua Hu, Lin Jiang

Abstract

In this paper, a novel beta parameter three-input one-output fuzzy-logic based maximum power point tracking (MPPT) algorithm is presented for the photovoltaic (PV) system application. The conventional fuzzy-logic controllers (FLCs) exhibit obvious limitations such as their dependence on the user's knowledge about the system and complicated rules. Furthermore, they show inherent dilemma between the rules number of FLC and the universality for various operating conditions, which is revealed and explained with details in this paper. Thus, a novel FLC is proposed by introducing a third input: an intermediate variable β. It can simplify the fuzzy rule membership functions and cover wider operating conditions. The dependence on the user's knowledge about the system is reduced. The converging speed for transients is improved and oscillations around the MPPs are completely eliminated compared with conventional MPPT methods. Typical operation conditions such as varying solar irradiation and load resistance are tested for fair comparison of various algorithms. An experimental prototype was designed and main experimental results were presented to verify the advantages of the proposed algorithm.

Index Terms

photovoltaic (PV) system, Maximum power point tracking (MPPT), fuzzy logic controller(FLC), beta parameter, zero oscillation.

I. Introduction

Since the output power of a PV system shows strong nonlinearity with respect to the irradiation and temperature, the maximum power point tracking (MPPT) techniques are usually adopted in the PV system to achieve the maximum power output from the installed PV modules under different conditions [13].

So far, many MPPT techniques have been used [10, 14, 35], such as Perturb and observe (P&O) [13, 15], Hill-Climbing (HC) [18] and incremental conductance (INC) [12, 32]. However, these techniques show obvious disadvantages, such as low tracking efficiency during rapidly changing solar irradiation and fluctuations around the maximum power points (MPPs) during the steady-state operation [34].

In order to improve the performance, many advanced MPPT algorithms have been proposed, such as the adaptive hill climbing [37], variable-step-size incremental conductance [25], and incremental resistance [27], have been proposed. However, the dilemma between the steady state and transient operations has not been solved perfectly [37]. The control implementation becomes complicated [27]. Additional parameters such as scaling factor are introduced and the optimal parameter must be determined firstly to ensure good performance [25]. Furthermore, there are still steady-state oscillations that could not be completely eliminated with these techniques.

In recent years, a number of MPTT algorithms without determination of step size are proposed to estimate the MPP rather than measure it. In [36], the weighted least square (WLS) function is used to estimate the MPP with three sampled points. Similarly, two different polynomial models are used to fit the I-V curve and obtain the MPP with three sampled points [8] and six sampled points [39], respectively. However, these model-based MPPT methods have a special requirement of the sampled points as well as a high computational load to estimate the MPP. Alternatively, a thermography-based MPPT method [16] and a optical-camera-based MPPT method [26] are proposed to estimate the MPP. However, these methods require additional hardware and they are not properly used in the real-time MPPT tracking.

Compared with aforementioned MPPT algorithms, Fuzzy-logic controllers (FLCs) is relatively simple and does not require any additional hardware requirement [38]. Besides, it can also exhibit faster tracking speed and more accurate steady-state performance [19, 33]. However, the conventional FLCs are heavily relied on the user's knowledge about the PV system and their rules are complicated [31]. Furthermore, FLC could not track the real MPPs when the irradiation changes quickly [4]. In order to overcome these drawbacks in FLC implementation, many researchers try to optimize the FLCs such as their membership functions (MFs) and fuzzy rules with the aid of the other artificial intelligence (AI) techniques, such as fuzzy cognitive networks [19], genetic algorithm [28], artificial neural network [9], particle swarm optimization [20] and adaptive network-based fuzzy inference system[1]. These AI techniques require designers deep knowledge in the practical implementation, which hinder the wide-use of these advanced FLC techniques.

To address this issue, a practical way is to combine the classical MPPT techniques, such as HC technique [4],P&O technique [30] and INC technique [31] with the FLCs in order to achieve easier MFs and fuzzy rules design. With the hybrid technique, faster converging speed for transients and less oscillation around the MPPs for the steady-state operation can be achieved [21]. The design of the FLC is simplified, for instance, the number of fuzzy rules can be reduced from 25 to 16 [4]. However, there is a dilemma between the rules number and the universality for various operating conditions. When the rules is simplified, the FLC will not track the MPPs successfully for some operating conditions. Thus, a

balance between the complexity of the rules and the universality of the algorithm must be achieved.

This paper will follow the principle of the hybrid MPPT techniques by introducing a variable β rather than the variation of the terminal voltage or the output power as the third input of FLC. It simplifies the fuzzy rule number and cover wider operating conditions. Both the static and dynamic performance can be improved. A PV system connected with boost converter was designed and the new FLC algorithm was implemented by the dSPACE. Simulation and experimental results for different scenarios are presented to demonstrate the advantages of the proposed MPPT algorithm in terms of fast converging speed and zero oscillation.

II. Conventional FLC MPPT Techniques

Fig. 1 shows the basic structure of FLCs, which are usually implemented with three stages: fuzzification, interference with rule base, and defuzzification [14]. Main function of the fuzzification is to convert the numerical input variables into equivalent linguistic variables as input fuzzy sets. The input fuzzy sets are then sent to the interference in order to obtain output fuzzy sets according to the fuzzy rule base table. Finally, the output of numerical variables can be obtained based on the output fuzzy sets.

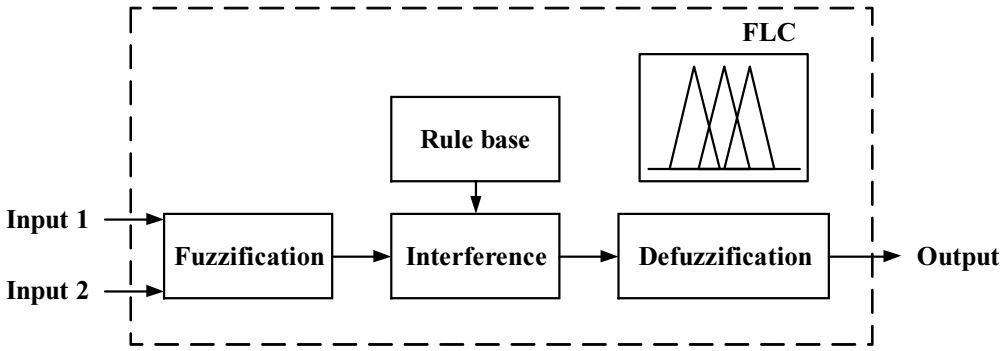

Fig. 1. Fuzzy logic controller.

For MPPT application, FLCs usually use Mamdani model for interference, Max-Min for fuzzy combination and center of gravity (COG) for defuzzification. The variations of the duty cycle (ΔD) is the output variable. The input variables are changed according to different FLC-based MPPT techniques. Normally, the error E and the change in error ΔE are acted as the the input variables [14]. The error E can be obtained by the slope of P-V curve as follow[5, 29]:

$$E(k) = \frac{P(k) - P(k-1)}{V(k) - V(k-1)} \tag{1}$$

$$\Delta E(k) = E(k) - E(k-1) \tag{2}$$

where $P(k)$ and $V(k)$ represent the PV output power and voltage respectively at the time instant k. Fig. 2 indicates that the instantaneous value of $E(k)$ is positive on the left or negative on the right of the MPP.

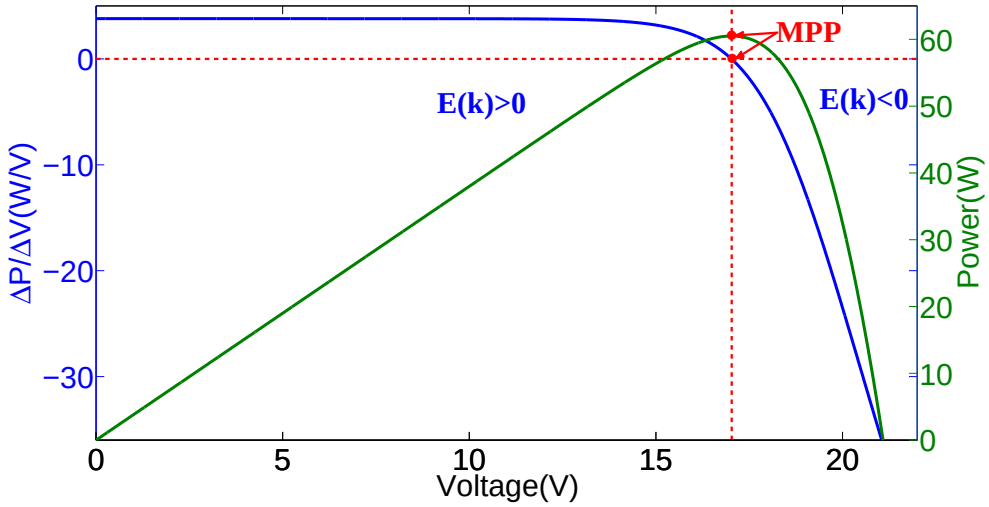

Fig. 2. Typical PV P-V and $\Delta P/\Delta V$ curves.

Normally the MFs of FLC-based MPPT techniques adopt five-fuzzy-level structure, including NB (negative big), NS (negative small), ZE (zero), PS (positive small), and PB (positive big). Since the curve of $\Delta P/\Delta V$ in Fig. 2 is highly asymmetric at the MPP, the MFs of $E(k)$ with five fuzzy levels have to be carefully designed in order to ensure the symmetry of the output variable ΔD [11]. The designed MFs with five fuzzy levels are demonstrated in Fig. 3, which shows that the output variable ΔD is symmetric around zero. The number of fuzzy rules is 25, which is high and will increase the difficult of FLC design and implementation. Although some artificial intelligence (AI) algorithms including fuzzy cognitive networks, genetic algorithm and particle swarm optimization can be used to optimize the MFs and fuzzy rules, these AI techniques themselves are complicated and require designers deep knowledge for these advanced AI algorithms.

Alternatively, some researchers try to integrate some classical MPPT techniques with the conventional FLC in order to achieve simple design of MFs and fuzzy rules. For instance, originated from the HC MPPT method, the research in [4] utilizes the variation of the output power (ΔP) and the variation of the output current (ΔI), instead of E and ΔE, as the input variables. Since this technique combines the HC with the fuzzy logic MPPT technique, it is called fuzzy-logic-based hill-climbing (FLC-HC). Similar hybrid MPPT algorithms, such as fuzzy-logic-based perturb and observe (FLC-P&O) and fuzzy-logic-based incremental conductance (FLC-INC) can be found in [30] and [31], respectively. In [30], the

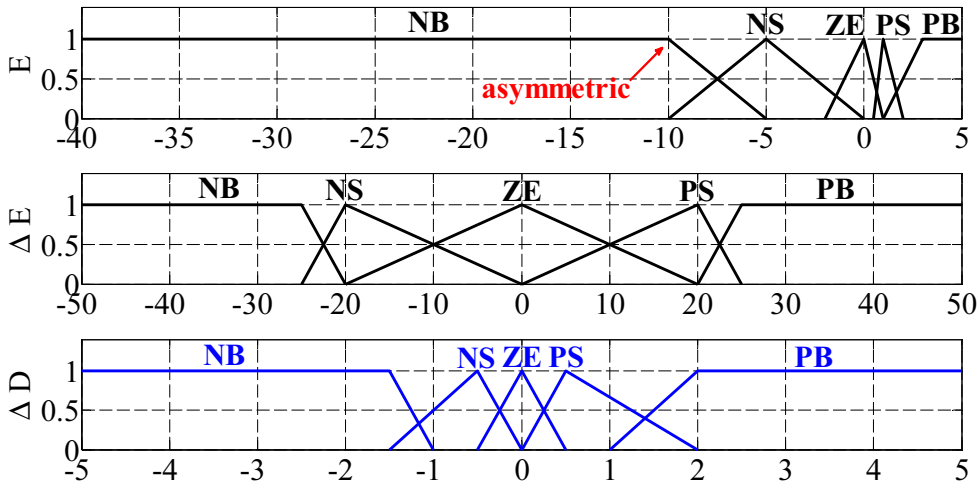

Fig. 3. Membership functions of five fuzzy levels.

incremental conductance e_{IC} is used for one of the input variables. These FLC techniques are summarised in TABLE I.

TABLE I
SUMMARISATION OF THE CONVENTIONAL FLC TECHNIQUES.

Ref.	Input variables	Output variables	Number of Rules	Inference mode	Converter type	Controller implementation
[4]	ΔP, ΔI	ΔD	16	Mamdani	Boost	Microchip Infineon TC1796
[30]	ΔP, ΔV	ΔD	25	Mamdani	Boost	DSP TMS320F28335
[31]	e_{IC}, ΔD	ΔD	9	Mamdani	Cuk	dSPACE
[29]	$\Delta P/\Delta V$	ΔD	25	Mamdani	Boost	FPGA V2MB1000
[5]	$\Delta P/\Delta V$	ΔD	25	Mamdani	Cuk	-
[3]	$\Delta P/\Delta V$, ΔD	ΔD	9	Mamdani	Buck	DSP TMS320F28335

The comparison is made among these MPPT algorithms in terms of the converging speed, steady oscillations, and the complexity in FLC implementation. For example, the method in [4] can reduce the number of fuzzy rules from 25 to 16. Using three fuzzy levels, such as small, medium and large, the method proposed in [3, 31] will further reduces to nine rules. However, for FLC algorithms, there is an inherent dilemma between the rules number and the universality for various operating conditions. For some conditions, some FLC algorithms show bad performance or even could not track the MPPs properly. This problem will be discussed in this paper and the corresponding reasons are explained properly.

Furthermore, all these FLC algorithms shown in TABLE I present significant steady oscillations.

III. Proposed Beta-Parameter based FLC MPPT Algorithm

A. Proposed scheme for the single peak tracking

Fig. 4 shows the basic structure of the proposed algorithm. The Mamdani model, Max-Min and COG are used for interference, fuzzy combination and defuzzification, respectively. Besides the variation of the output power (ΔP) and the variation of the output voltage (ΔV), a third input variable β is introduced. The variation of the duty cycle is the output.

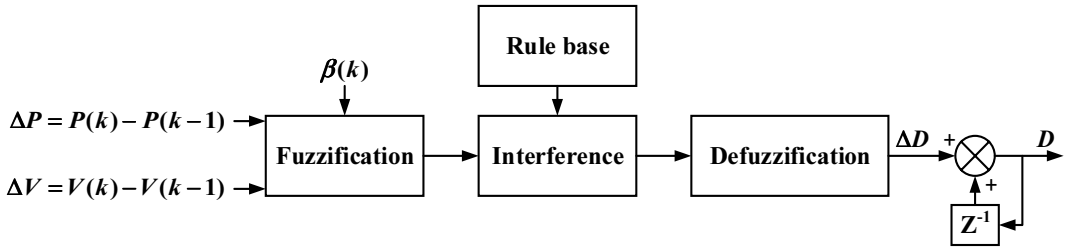

Fig. 4. Proposed FLC Algorithm.

TABLE II

Values of β under various working conditions

No.	Irradiance	temperature	β
1	1000 W/m^2	45°C	-15.4505
2	1000 W/m^2	5°C	-18.3431
3	300 W/m^2	45°C	-15.9587
4	300 W/m^2	5°C	-19.0214

The beta-parameter based MPPT algorithm was proposed by [17] and the newly added variable β is expressed by:

$$\beta = ln\Big(\frac{I}{V}\Big) - c \times V \tag{3}$$

where V and I represents the PV voltage and current, c is the function of cell number, temperature, and the diode structure [17].

In this algorithm, a range of (β_{min}, β_{max}) is defined, which depends on the practical environmental conditions, such as the irradiance and temperature [23]. The parameter β is continuously monitored to

determine if it is located within the defined range. If β is located within this range, it indicates that the operating point is close to the true MPP. TABLE II illustrates the calculated magnitudes of β for different environmental conditions. Fig. 5 shows that the the range of β is narrow for a wide working conditions, which facilitate the dynamic tracking. In [24], two sets of the distinguished meteorological data are used to evaluate the effectiveness of the range of β. Generally, the range of β should be determined by the local meteorological data under the extreme conditions, such as extreme temperature and solar irradiance.

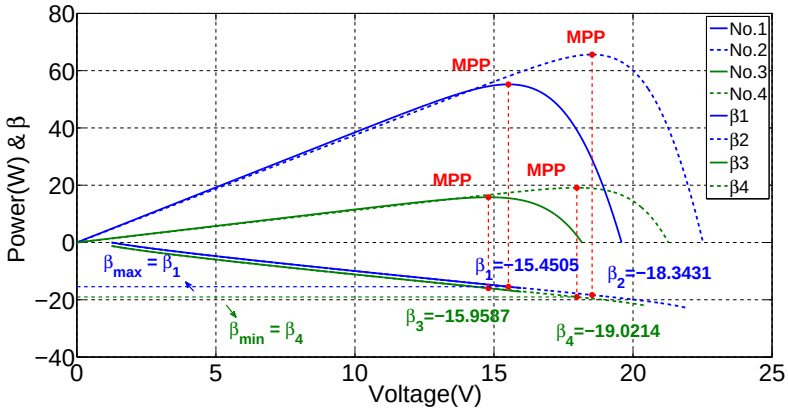

Fig. 5. Range of β and power under various irradiance and temperature conditions.

With the proposed algorithm, Fig. 6 and TABLE III shows the membership functions and fuzzy rules. Three fuzzy sets, β_{min}, β_{mid}, and β_{max}, are used with respect to the variable β. TABLE III shows the fuzzy rules for the proposed MPPT technique. The output is either PB for β_{min} and or NB for β_{max} respectively, which is independent on the value of ΔP and ΔV. For β_{mid}, there are three possible fuzzy subsets: NS, ZE, and PS. Thus, there are totally only 11 rules required for the proposed FLC algorithm, which is much less than other FLCs. Compared with the FLC-HC, it covers wider operating conditions. Furthermore, the output shows relatively symmetric feature, as illustrated in Fig. 6, which further simplify the algorithm implementation.

The detailed tracking process with the proposed algorithm is illustrated in Fig.7. The irradiance is set as follows: the irradiance is firstly set as 1000 W/m^2. At t=0.5 s, the irradiance decreases to 400 W/m^2. The movement of the operating point can be explained as: firstly, the PV module operates at point A, which is the MPP for 1000 W/m^2, as shown in Fig.7 (a). At this time, the fuzzy input parameter β is β_{mid} and the other input parameters, ΔP and ΔV, are ZE. According to TABLE III, the output ΔD is ZE as shown in Fig.7 (b). For the irradiance change at $t = 0.5s$, the operating point will still locate at the load line 1 considering that the duty cycle of the power converter remains unchanged at that moment. Specifically, the operating point switches immediately from A to B, which is the intersection

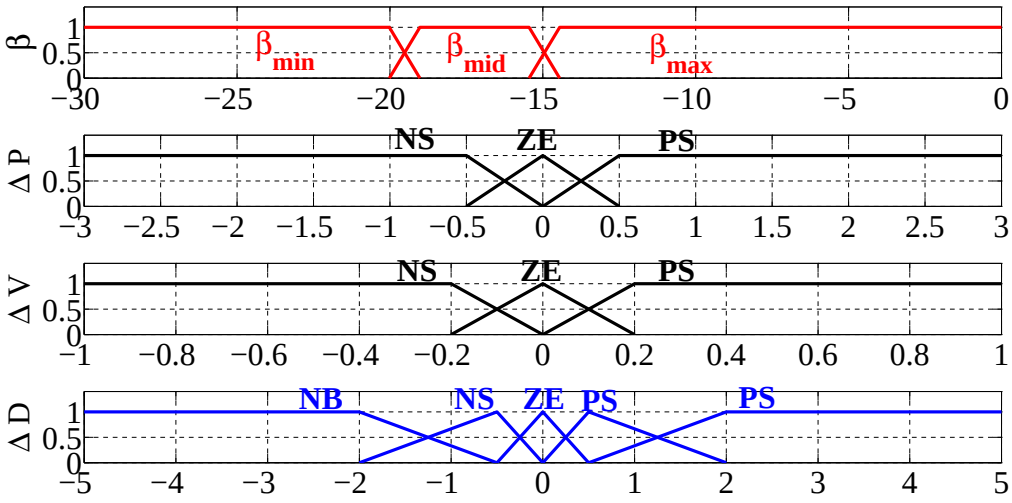

Fig. 6. MFs of the proposed FLC.

TABLE III

FUZZY RULES OF THE PROPOSED FLC

β_{min}	PB			
β_{mid}	ΔP \ ΔV	NS	ZE	PS
	NS	NS	ZE	PS
	ZE	ZE	ZE	ZE
	PS	PS	ZE	NS
β_{max}	NB			

point between the load line 1 and the I-V curve for 400 W/m^2. Then, β is found as β_{max}, so ΔD is NB regardless of ΔP and ΔV according to TABLE III. At $t = 0.6s$, β is equal to β_{mid} and both of ΔP and ΔV are equal to PS, as illustrated in Fig.7 (b). Consequently, ΔD is equal to NS. After several iteration, both of ΔP and ΔV are equal to ZE, so ΔD is stabilized to ZE. Thus, point C is finally located for the steady state operation and the zero oscillation is realized. Fig.7 (c) illustrates the case for the irradiance increase, which shows similar process.

B. Possible extensions to the multiple peaks tracking

In practice, a PV string (or a PV array) rather than a PV module is generally used. When the PV string is partially shaded, there will be multiple peaks rather than a single peak for its corresponding I–V curve. Some of the MPPT methods may be affected since these MPPT methods are unable to distinguish

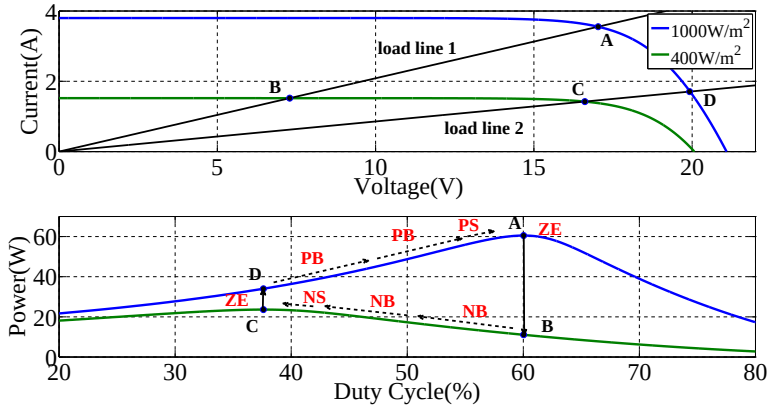

(a)

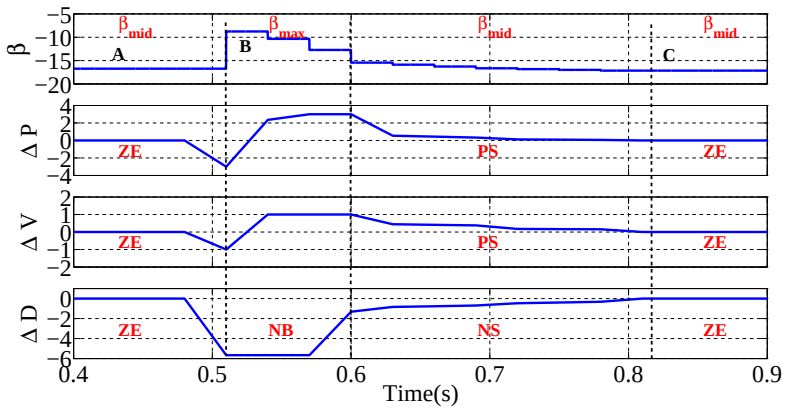

(b)

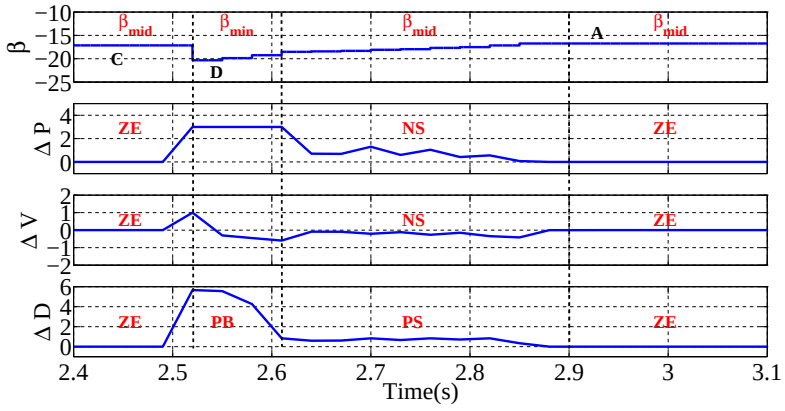

(c)

Fig. 7. Dynamic tracking process with the proposed FLC. (a)I-V and P-D curves; (b)Fuzzy parameters for the proposed technique when the irradiance decreases; (c)changes of the fuzzy parameters for the proposed technique when the irradiance increases.

the global MPP (GMPP) from the local MPPs (LMPP). However, the proposed method is also possible to extended for this multiple-peak tracking. The key of this possible extensions is how to convert one multiple-peak curve into several single-peak curves [22].

In [6, 7], it was pointed out the I–V curve of a PV string is always determined by one key module since other modules are approximately constant or linear. Therefore, an explicit functions of the equivalent values of voltage (V_{eq}) of this key module is expressed as [22]:

$$V_{eq} = V_{String} - (n-1) \times V_s + (m-n) \times V_d \tag{4}$$

$$V_s \approx \frac{V_{MPP,stc} - V_{oc,stc}}{I_{MPP,stc}} \times I_{String} + V_{oc,stc} \tag{5}$$

$$n = 1, 2...m, for (m-1) \cdot \alpha \cdot V_{oc} < V_{String} <= m \cdot \alpha \cdot V_{oc} \tag{6}$$

where V_{String} and I_{String} represent the output voltage and current of the PV string, respectively; V_d refers to the constant value while V_s refers to the linear source as expressed in (5); m refers to the total number of PV modules in the PV string, and n is determined by (6); V_{oc} is the open-circuit voltage of PV modules, $V_{MPP,stc}$ and $I_{MPP,stc}$ represent voltage and current at the MPP under the standard test condition (STC), respectively; α is a variable that is varying from 0.8 to 0.97 [2].

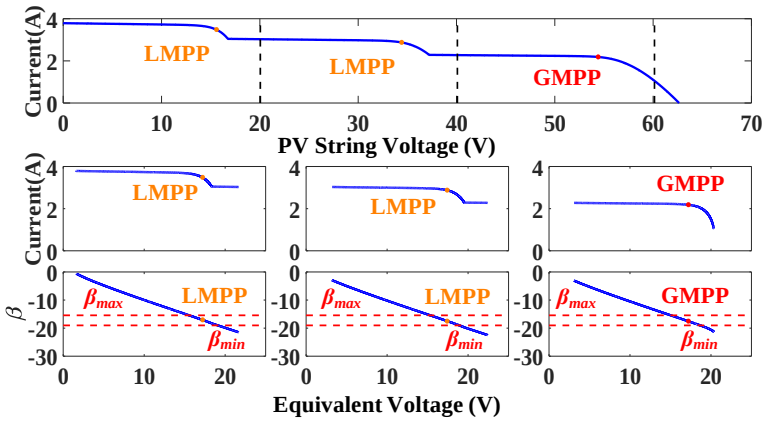

Fig. 8. I-V curves for the PV string with the multiple peaks and its equivalent values of voltage and β.

Substitute (4-6) into (3), the equivalent value of β, β_{eq}, can be determined. As a consequence, the I-V curves for the PV string with the multiple peaks and its equivalent values of voltage and β is shown in Fig.8. As shown in Fig.8, the whole I-V curves for the PV string is converted into three single-peak curves. Then, the each single-peak curve can be individually tracked by the proposed method and the possible extensions of the proposed method is shown in Fig.9.

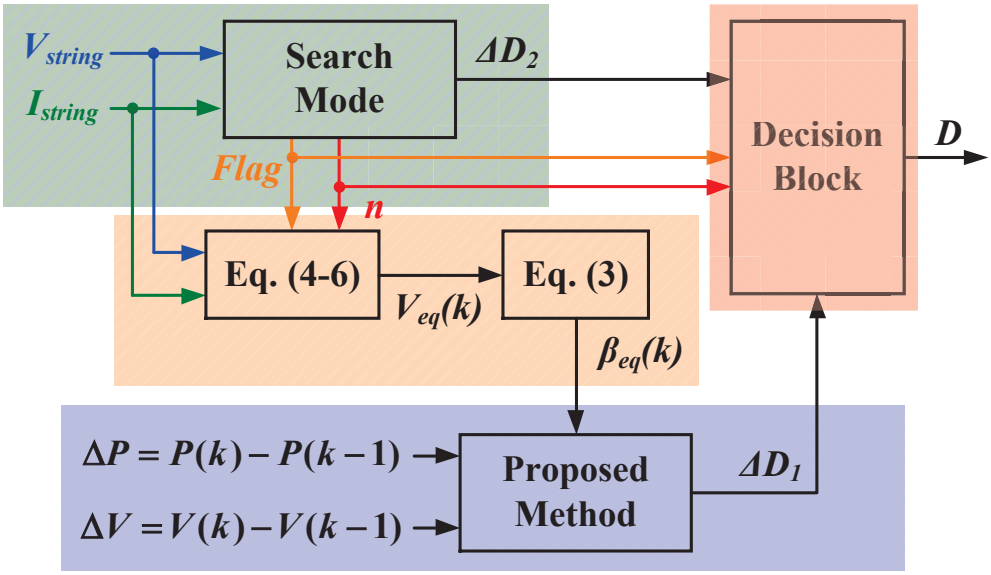

Fig. 9. Possible extensions of the proposed method for the multiple-peak tracking.

As shown in Fig.9, the proposed method, such as membership functions and fuzzy rules, is remained. One of the input parameter for the proposed method, $\beta(k)$, is changed to $\beta_{eq}(k)$, which is determined by (4-6). The step size generated by the proposed method ΔD_1 is used to track each single-peak curve and the step size generated by the search mode ΔD_2 is used to move the operating point from one peak to another. Finally, the decision block decides to new step size is ΔD_1 or ΔD_2. The details related to the search mode and decision block could be found in [22].

Although the proposed method could be extended to use for multiple-peak tracking, this paper will not validate this possibility since it is out of scope.

IV. Simulation Analysis

Fig.10 shows the simulation model with main components such as the PV module, boost converter with the proposed FLC and load. Main parameters for the PV modules, MSX-60W are: maximum power is 60 W, the voltage and current at the maximum power are 17.1 V and 3.5 A, open-circuit voltage is 21.1 V, and the short-circuit current is 3.8 A. TABLE IV lists main parameters for the boost converter. The MatLab/Simulink sub-model for the proposed MPPT technique is shown in Fig.11. The sampling time for the MPPT algorithm, T_p, is set as 0.03 s.

In order to comprehensively evaluate the performance of the proposed technique, typical MPPT techniques such as P&O technique [15], FLC-HC technique [4], and the proposed algorithm are tested.

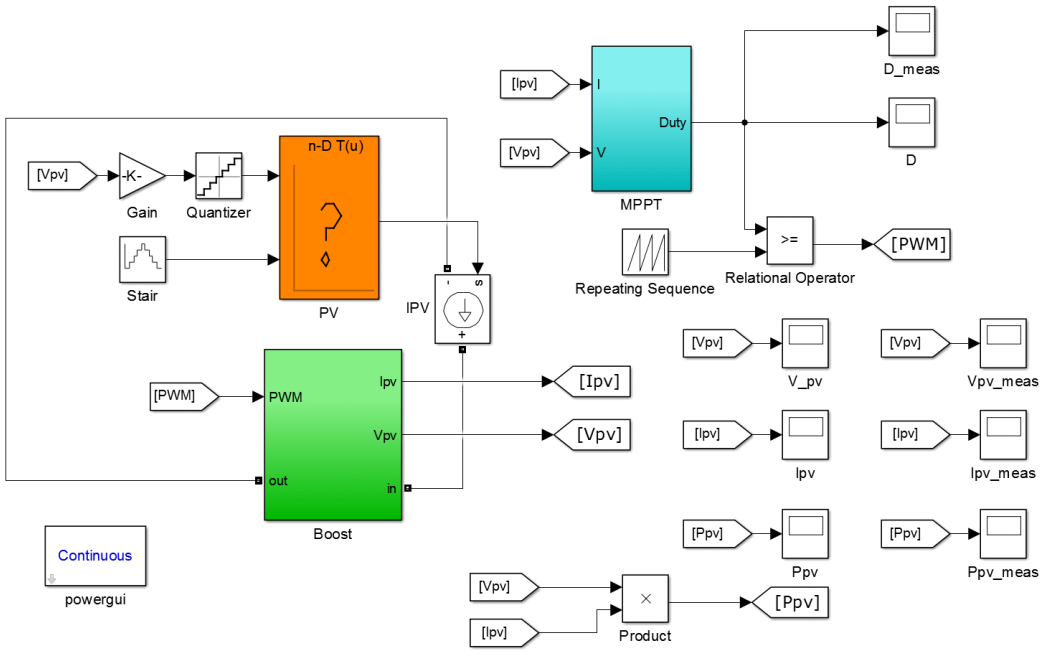

Fig. 10. Simulation model of PV system with MPPT control in MatLab/Simulink

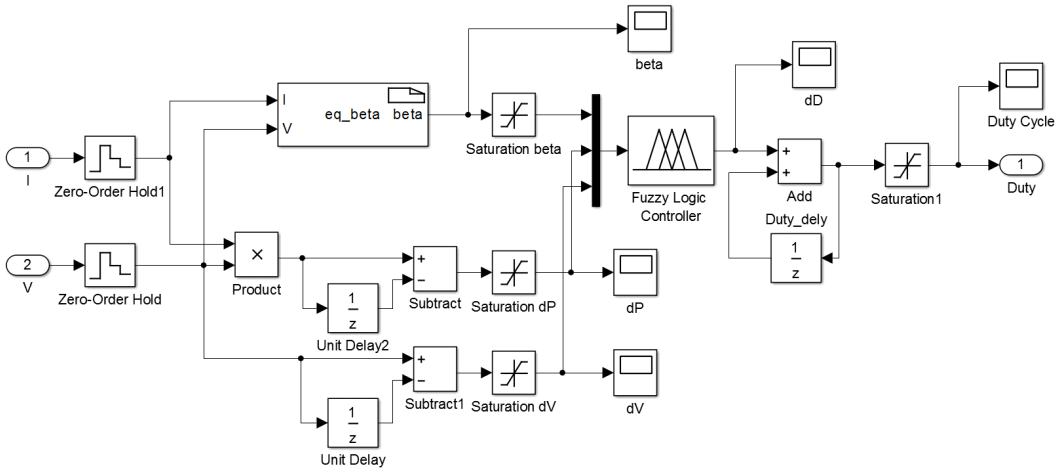

Fig. 11. Proposed MPPT technique with FLC in MatLab/Simulink.

Three different scenarios are considered, including the strong-intensity irradiance change, the weak-intensity irradiance change, and the load change.

A. Scenario One: Strong-intensity irradiance change

The scenario of strong-intensity irradiance change is defined that the irradiance changes between $1000W/m^2$ and $600W/m^2$. At t=0.5 s, the irradiance level is decreased to 600 W/m^2. At t=2 s, it will

TABLE IV

MAIN PARAMETERS OF THE BOOST CONVERTER

Parameter	Symbol	Value
PV side input capacitance	C_{in}	470 uF
Output capacitance	C_{out}	47 uF
Inductance	L	1 mH
Switching frequency (IGBT)	f_{sw}	10 kHz

return back to 1000 W/m^2 . For this scenario, R_{load} is fixed at 30 Ω.

Fig.12 shows main simulation results. It indicates that P&O needs longest time to find the true MPPT and then followed by the FLC-HC algorithm. The steady-state oscillations with both algorithm can be easily observed. Thus, the static power loss is increased. Besides, Fig.12 (b) shows that the FLC-HC shows the divergence from the real MPP when the irradiance decreases. The proposed FLC takes the shortest time among the three algorithms. Furthermore, Fig.12 (c) shows no divergence and zero steady-state oscillation.

B. Scenario Two: Weak-intensity irradiance change

The scenario of strong-intensity irradiance change is defined that the irradiance changes between 400 W/m^2 and 100 W/m^2. At t=1 s, the irradiance level is decreased to 100 W/m^2. At t=4 s, it will return back to 400 W/m^2 . For this scenario, R_{load} is fixed at 80 Ω, which represents low-power operating region.

Fig.13 shows main simulation results. Among these algorithms, the proposed technique requires shortest time to find the real MPP. Fig.13 (b) indicates that FLC-HC technique could not find the real MPP for this scenario with $100W/m^2$ irradiance. This can be explained by the detailed tracking process of FLC-HC algorithm, which is shown in Fig.14. At time t = 1 s, the irradiance decreases from 400 W/m^2 to 100 W/m^2 and the operating point moves from point E to F. Since both of ΔP and ΔI are NB, ΔD is equal to PB according to the rule table of FLC-HC [4]. However, this results in the divergence from the MPP, as illustrated in Fig.14. Furthermore, since the point F is located around the I_{sc}, both of ΔP and ΔI are always NS. Therefore, the output ΔD is always equal to NS, which results in a slow tracking speed [4].

C. Scenario Three: Load change

This scenario is defined that R_{load} changes between 60 Ω and 30 Ω. At t=0.5 s, R_{load} is decreased to 30 Ω. At t=2 s, it will return back to 60 Ω. During this period, the irradiance is fixed at 600 W/m^2.

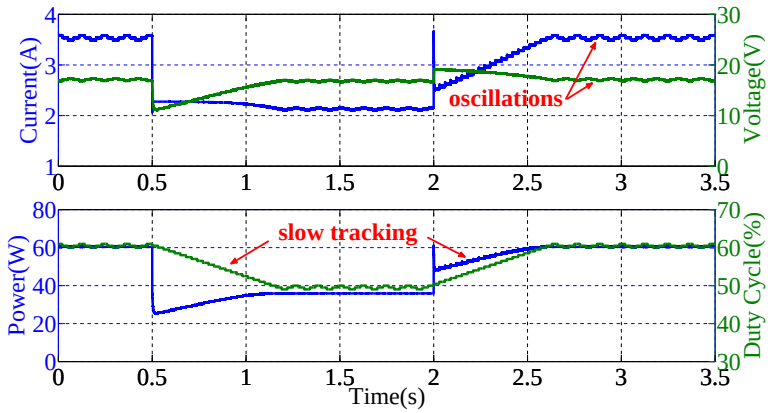

(a)

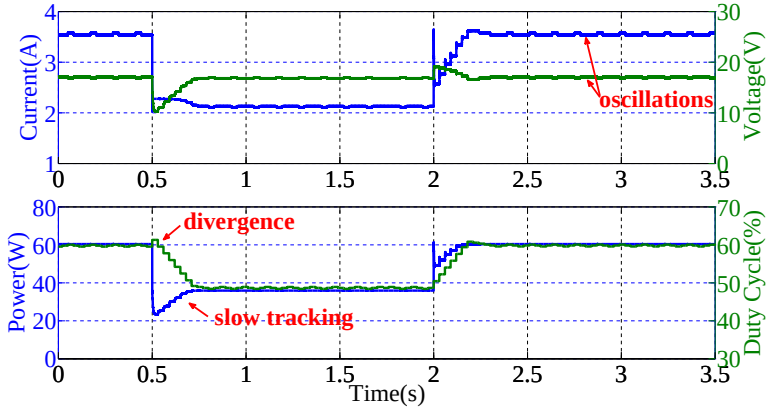

(b)

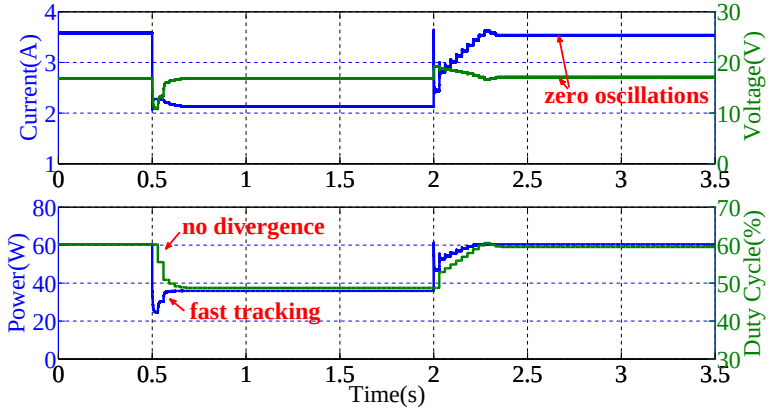

(c)

Fig. 12. Simulation results for the Scenario One. (a)P&O technique; (b)FLC-HC technique; (c)the proposed technique.

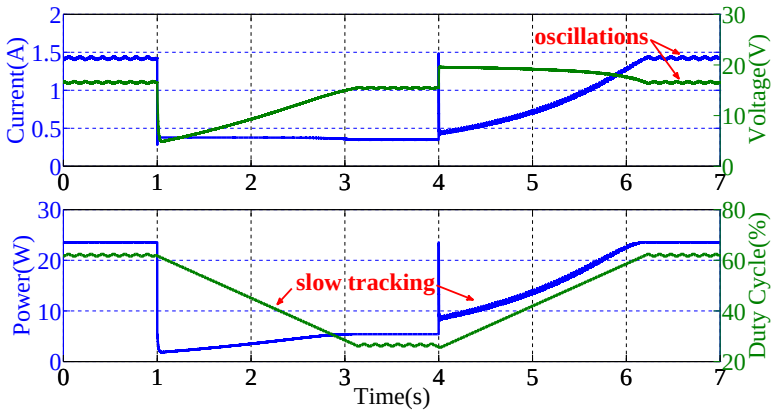

(a)

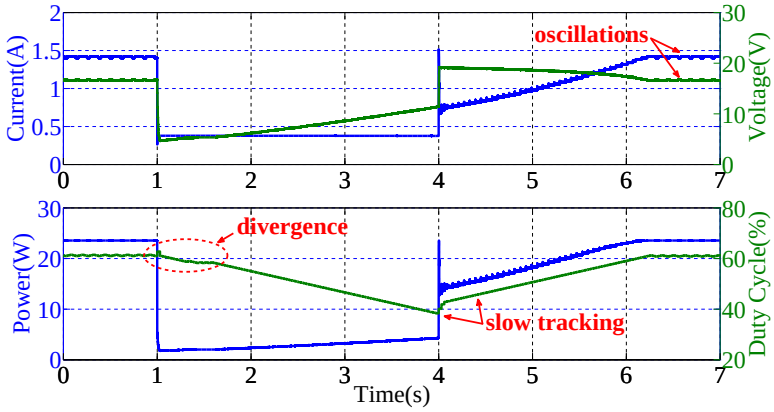

(b)

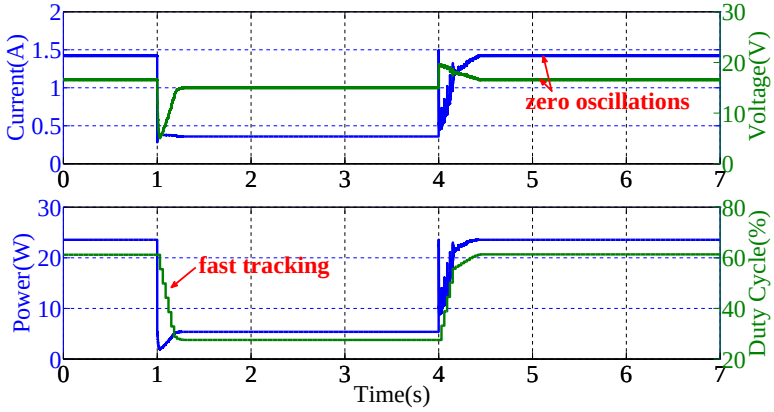

(c)

Fig. 13. Simulation results for the Scenario Two. (a)P&O technique; (b)FLC-HC technique; (c)the proposed technique.

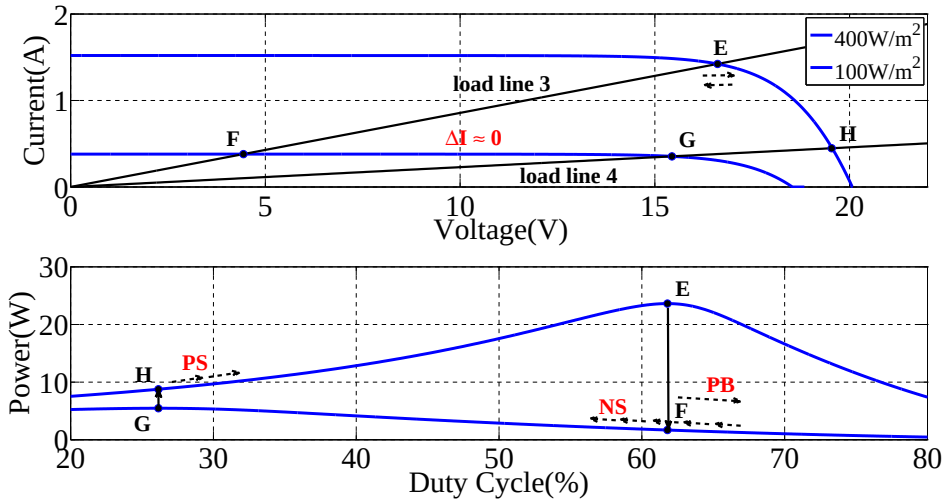

Fig. 14. Simulation results by using the FLC-HC technique.

Fig.15 shows main simulation results. Fig.15 shows that the proposed FLC requires least time to determine the real MPP while P&O requires longest time, as shown in Fig.15. This conclusion is similar with that of previous two scenarios. Furthermore, Fig.12 shows no divergence and zero static oscillations.

V. Experimental Results

Experimental tests on a prototype were conducted in order to verify the advantages of the proposed FLC. Fig.16 shows the test bench of this PV system, including main components such as PV emulator Chroma ATE-62050H-600S, boost converter, dSPACE DS1104 controller, and electronic load IT8514C+. The parameters of boost converter were set the same as the simulation. Three scenarios were evaluated and their parameter setting was set the same as the simulation.

Fig.17 shows main experimental waveforms, including the output power, current and voltage from the PV emulator under the Scenario One. It shows that the proposed FLC requires the least time to determine the real MPP among all these three algorithms. No steady oscillations were observed with the proposed FLC while the steady-static oscillations with other algorithms are easily observed.

Fig.18 shows the experimental results for the Scenario Two. The proposed FLC exhibits the least tracking time, the lowest tracking power loss, and zero oscillations among these MPPT techniques. The FLC-HC technique is unable to track the MPP under this scenario and the PV voltage could not reach the new steady state due to the irradiation variation, as illustrated in Fig.18(b). Obvious oscillation in voltage and current waveforms are observed. This phenomenon that FLC-HC could not track the MPP

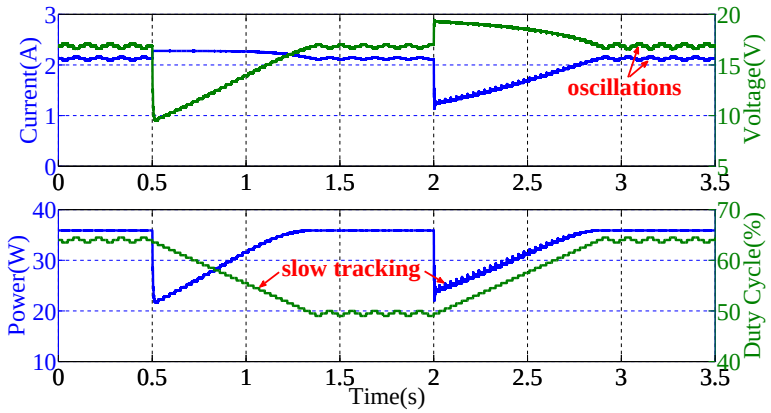

(a)

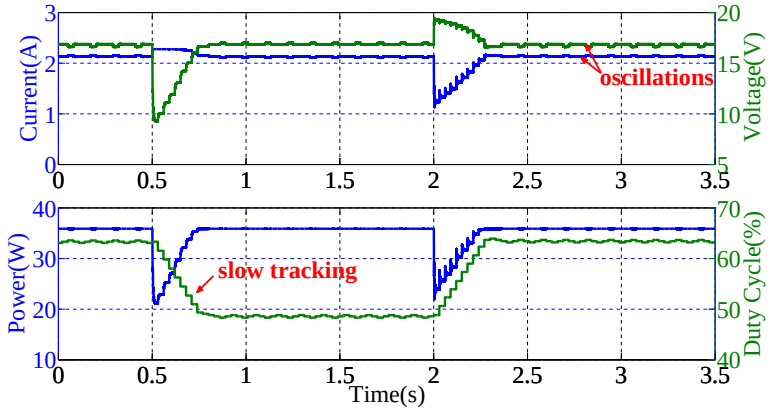

(b)

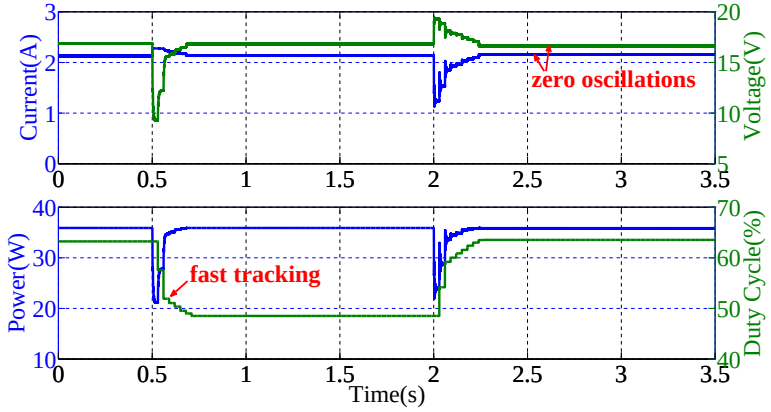

(c)

Fig. 15. Simulation results for the Scenario Three. (a)P&O technique; (b)FLC-HC technique; (c)the proposed technique.

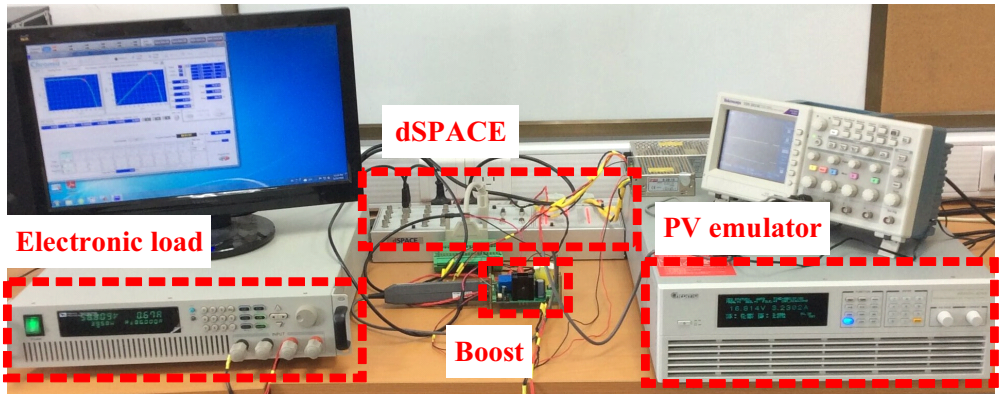

Fig. 16. Experimental prototype.

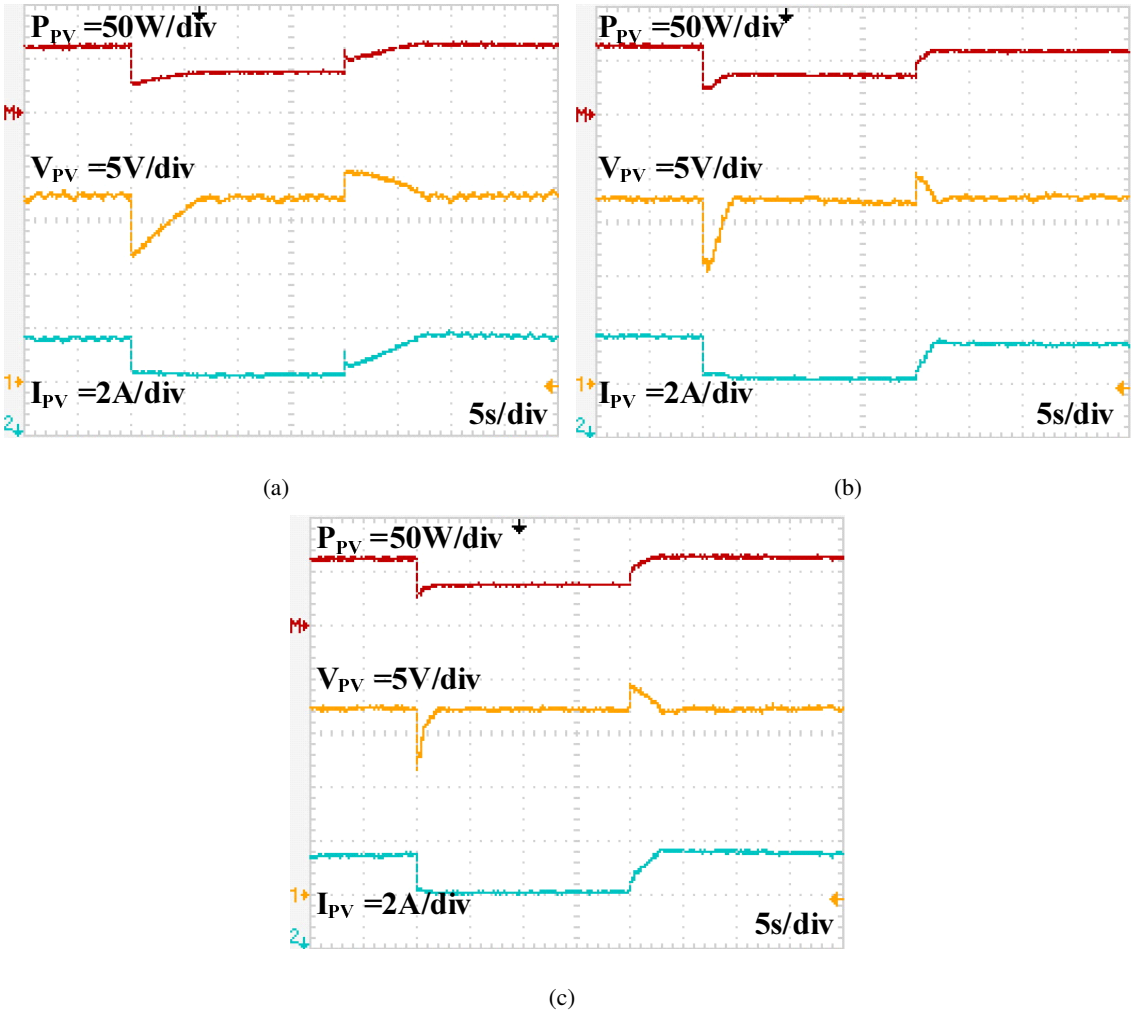

Fig. 17. Experimental results for the Scenario One. (a)P&O technique; (b)FLC-HC technique; (c)the proposed technique.

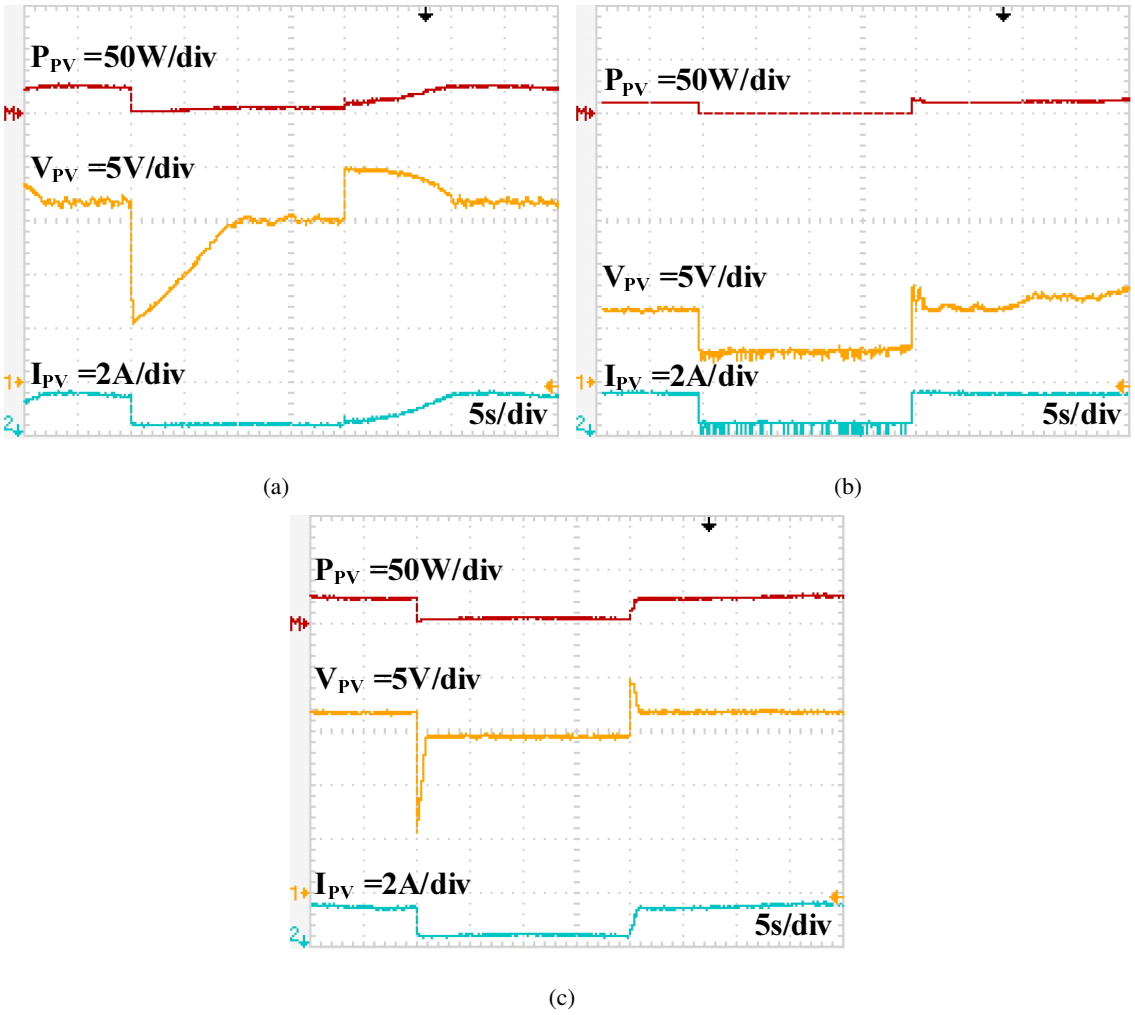

Fig. 18. Experimental results for the Scenario Two. (a)P&O technique; (b)FLC-HC technique; (c)the proposed technique.

under low irradiation conditions has been explained in Fig.14 of section VI. For the P&O technique, the static voltage oscillations are easily observed especially for the low irradiance condition of 100 W/m^2.

Fig.19 illustrates the experimental results for the Scenario Three. The proposed FLC shows faster responses than the other methods and zero oscillate for the steady-state operation.

VI. Conclusion

This paper proposed a novel FLC MPPT algorithm with β parameter. It's new three-inputs one-output fuzzy-logic controller by introducing an intermediate variable β as the input variable. The dilemma between the rules number and the universality for various operating conditions can be effectively solved with this new algorithm. It can simplify the Fuzzy rule membership functions since the number of fuzzy rules can be reduced to 11. Furthermore, this algorithm can be used for various operating conditions

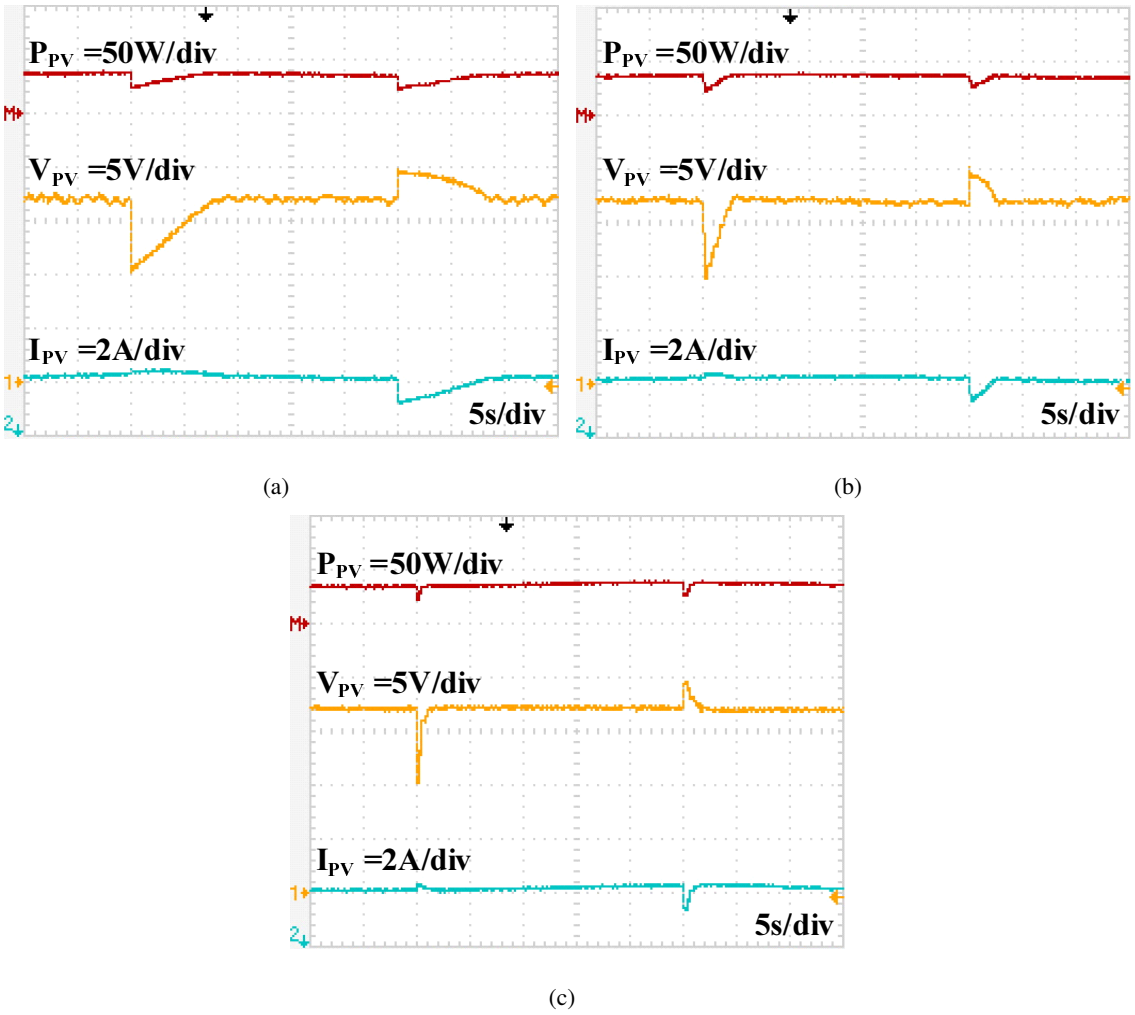

Fig. 19. Experimental results for the Scenario Three. (a)P&O technique; (b)FLC-HC technique; (c)the proposed technique.

especially for rapidly changing environmental conditions and low irradiation conditions, where the FLC-HC could not track the real MPPs successfully. The dependency of this method on the designer's knowledge of the system is reduced by using the new algorithm since the intermediate variable β can be directly calculated from the measured voltage and current for each sampling period. The converging speed for transients is improved by comparison with other MPPT methods. Oscillations around the MPPs are completely eliminated for steady-state operations. Various scenarios are analyzed and simulated according to the irradiance change and load variation. Simulation and experimental results were provided, which verified the advantages of the proposed FLC algorithm.

ACKNOWLEDGMENT

This research was supported by University Research Development Fund (RDF-16-01-10), the Suzhou Prospective Application Programme (SYG201723), the Jiangsu Science and Technology Programme (BK20161252), and the National Nature Science Foundation of China (51407145).

VII. REFERENCE

REFERENCES

[1] Abu-Rub, H., Iqbal, A., Moin Ahmed, S., Peng, F. Z., Yuan, L., Ge, B., 2013. Quasi-z-source inverter-based photovoltaic generation system with maximum power tracking control using anfis. IEEE Trans. Sustain. Energy 4 (1), 11–20.

[2] Ahmed, J., Salam, Z., Dec. 2015. An improved method to predict the position of maximum power point during partial shading for pv arrays. IEEE Trans. Ind.l Informat. 11 (6), 1378–1387.

[3] Al Nabulsi, A., Dhaouadi, R., Aug. 2012. Efficiency optimization of a dsp-based standalone pv system using fuzzy logic and dual-mppt control. IEEE Trans. Ind. Informat. 8 (3), 573–584.

[4] Alajmi, B., Ahmed, K. H., Finney, S. J., Williams, B. W., Apr. 2011. Fuzzy-logic-control approach of a modified hill-climbing method for maximum power point in microgrid standalone photovoltaic system. IEEE Trans. Power Electron. 26 (4), 1022–1030.

[5] Algazar, M. M., Al-monier, H., El-halim, H. A., Salem, M. E. E. K., 2012. Maximum power point tracking using fuzzy logic control. Int. J. Elec. Power 39 (1), 21–28.

[6] Batzelis, E. I., Kampitsis, G. E., Papathanassiou, S. A., Manias, S. N., Mar. 2015. Direct mpp calculation in terms of the single-diode pv model parameters. IEEE Trans. Energy Convers. 30 (1), 226–236.

[7] Batzelis, E. I., Routsolias, I. A., Papathanassiou, S. A., Jan. 2014. An explicit pv string model based on the lambert w function and simplified mpp expressions for operation under partial shading. IEEE Trans. Sustain. Energy 5 (1), 301–312.

[8] Blanes, J. M., Toledo, F. J., Montero, S., Garrigs, A., Mar. 2013. In-site real-time photovoltaic i-v curves and maximum power point estimator. IEEE Trans. Power Electron. 28 (3), 1234–1240.

[9] Chaouachi, A., Kamel, R. M., Nagasaka, K., 2010. A novel multi-model neuro-fuzzy-based mppt for three-phase grid-connected photovoltaic system. Sol. Energy 84 (12), 2219–2229.

[10] de Brito, M., Galotto, L., Sampaio, L., de Azevedo e Melo, G., Canesin, C., Mar. 2013. Evaluation of the main mppt techniques for photovoltaic applications. IEEE Trans. Ind. Electron 60 (3), 1156–1167.

[11] El Khateb, A., Abd Rahim, N., Selvaraj, J., Uddin, M., Jul. 2014. Fuzzy-logic-controller-based sepic converter for maximum power point tracking. IEEE Trans. Ind. Appl. 50 (4), 2349–2358.

[12] Elgendy, M., Zahawi, B., Atkinson, D., Jan. 2013. Assessment of the incremental conductance maximum power point tracking algorithm. IEEE Trans. Sustain. Energy 4 (1), 108–117.

[13] Elgendy, M., Zahawi, B., Atkinson, D., Mar. 2015. Operating characteristics of the p amp;o algorithm at high perturbation frequencies for standalone pv systems. IEEE Trans. Energy Convers. 30 (1), 189–198.

[14] Esram, T., Chapman, P., Jun. 2007. Comparison of photovoltaic array maximum power point tracking techniques. IEEE Trans. Energy Convers. 22 (2), 439–449.

[15] Femia, N., Petrone, G., Spagnuolo, G., Vitelli, M., Jul. 2005. Optimization of perturb and observe maximum power point tracking method. IEEE Trans. Power Electron. 20 (4), 963–973.

[16] Hu, Y., Cao, W., Wu, J., Ji, B., Holliday, D., Nov. 2014. Thermography-based virtual mppt scheme for improving pv energy efficiency under partial shading conditions. IEEE Trans. Power Electron. 29 (11), 5667–5672.

[17] Jain, S., Agarwal, V., Mar. 2004. A new algorithm for rapid tracking of approximate maximum power point in photovoltaic systems. IEEE Power Electron. Lett. 2 (1), 16–19.

[18] Kjaer, S., Dec. 2012. Evaluation of the hill climbing and the incremental conductance maximum power point trackers for photovoltaic power systems. IEEE Trans. Energy Convers. 27 (4), 922–929.

[19] Kottas, T. L., Boutalis, Y. S., Karlis, A. D., Sep. 2006. New maximum power point tracker for pv arrays using fuzzy controller in close cooperation with fuzzy cognitive networks. IEEE Trans. Energy Convers. 21 (3), 793–803.

[20] Letting, L. K., Munda, J. L., Hamam, Y., 2012. Optimization of a fuzzy logic controller for pv grid inverter control using s-function based pso. Sol. Energy 86 (6), 1689–1700.

[21] Li, X., Wen, H., 2016. A fuzzy logic controller with beta parameter for maximum power point tracking of photovoltaic systems. In: 2016 IEEE 8th International Power Electronics and Motion Control Conference (IPEMC-ECCE Asia). pp. 1550–1555.

[22] Li, X., Wen, H., Hu, Y., Jiang, L., Xiao, W., Mar. 2018. Modified beta algorithm for gmppt and partial shading detection in photovoltaic systems. IEEE Trans. Power Electron. 33 (3), 2172–2186.

[23] Li, X., Wen, H., Jiang, L., Hu, Y., Zhao, C., Sep. 2016. An improved beta method with auto-scaling factor for photovoltaic system. IEEE Trans. Ind. Appl. 52 (5), 4281–4291.

[24] Li, X., Wen, H., Jiang, L., Xiao, W., Du, Y., Zhao, C., Nov. 2016. An improved mppt method for pv system with fast-converging speed and zero oscillation. IEEE Trans. Ind. Appl. 52 (6), 5051–5064.

[25] Liu, F., Duan, S., Liu, F., Liu, B., Kang, Y., Jul. 2008. A variable step size inc mppt method for

pv systems. IEEE Trans. Ind. Electron. 55 (7), 2622–2628.

[26] Mahmoud, Y., El-Saadany, E. F., Mar. 2017. A novel mppt technique based on an image of pv modules. IEEE Trans. Energy Convers. 32 (1), 213–221.

[27] Mei, Q., Shan, M., Liu, L., Guerrero, J., Jun. 2011. A novel improved variable step-size incremental-resistance mppt method for pv systems. IEEE Trans. Ind. Electron 58 (6), 2427–2434.

[28] Messai, A., Mellit, A., Guessoum, A., Kalogirou, S. A., 2011. Maximum power point tracking using a ga optimized fuzzy logic controller and its fpga implementation. Sol. Energy 85 (2), 265–277.

[29] Messai, A., Mellit, A., Massi Pavan, A., Guessoum, A., Mekki, H., 2011. Fpga-based implementation of a fuzzy controller (mppt) for photovoltaic module. Energy Convers. Manage. 52 (7), 2695–2704.

[30] Mohd Zainuri, M., Mohd Radzi, M., Soh, A., Rahim, N., 2014. Development of adaptive perturb and observe-fuzzy control maximum power point tracking for photovoltaic boost dc-dc converter. IET Renew. Power Gen. 8 (2), 183–194.

[31] Radjai, T., Rahmani, L., Mekhilef, S., Gaubert, J. P., 2014. Implementation of a modified incremental conductance mppt algorithm with direct control based on a fuzzy duty cycle change estimator using dspace. Sol. Energy 110, 325–337.

[32] Safari, A., Mekhilef, S., Apr. 2011. Simulation and hardware implementation of incremental conductance mppt with direct control method using cuk converter. IEEE Trans. Ind. Electron 58 (4), 1154–1161.

[33] Simoes, M. G., Franceschetti, N. N., Sep. 1999. Fuzzy optimisation based control of a solar array system. IEE Proc. Electr. Power Appl. 146 (5), 552558.

[34] Soon, T. K., Mekhilef, S., 2014. Modified incremental conductance mppt algorithm to mitigate inaccurate responses under fast-changing solar irradiation level. Sol. Energy 101 (0), 333 – 342.

[35] Subudhi, B., Pradhan, R., Jan. 2013. A comparative study on maximum power point tracking techniques for photovoltaic power systems. IEEE Trans. Sustain. Energy 4 (1), 89–98.

[36] Teng, J. H., Huang, W. H., Hsu, T. A., Wang, C. Y., Aug. 2016. Novel and fast maximum power point tracking for photovoltaic generation. IEEE Trans. Ind. Electron. 63 (8), 4955–4966.

[37] Xiao, W., Dunford, W., Jun. 2004. A modified adaptive hill climbing mppt method for photovoltaic power systems. In: Proc. 2004 IEEE 35th Annu. Power Electron. Spec. Conf. Vol. 3. pp. 1957–1963 Vol.3.

[38] Yilmaz, U., Kircay, A., Borekci, S., Jan. 2018. Pv system fuzzy logic mppt method and pi control as a charge controller. Renew. Sust. Energ. Rev. 81, 994–1001.

[39] Zadeh, M. J. Z., Fathi, S. H., Dec. 2017. A new approach for photovoltaic arrays modeling and maximum power point estimation in real operating conditions. IEEE Trans. Ind. Electron. 64 (12),

9334–9343.